Spectroscopic and Electrochemical Characterization of 18-Molybdodisulfate(VI)(4−), $S_2Mo_{18}O_{62}^{4-}$

Sadayuki HIMENO,* Toshitaka HORI,† and Atsuyoshi SAITO
Department of Chemistry, College of Liberal Arts, Kobe University, Kobe 657
†Department of Chemistry, College of Liberal Arts and Sciences, Kyoto University, Kyoto 606
(Received October 13, 1988)

The formation conditions of a yellow Dawson-type $S_2Mo_{18}O_{62}^{4-}$ anion have been investigated as functions of the concentrations of Mo(VI), H_2SO_4, organic solvents, the nature of the organic solvents used, temperature of the solution, and the reaction time. For a 50 mM Mo(VI)/50% (v/v) acetonitrile system, the yellow $S_2Mo_{18}O_{62}^{4-}$ anion formed in 0.2—1.0 M H_2SO_4, while a pale-yellow $Mo_6O_{19}^{2-}$ anion did in 0.04—0.3 M H_2SO_4. The yellow heteropolyanion is electrochemically reduced in six successive steps to mixed-valence heteropoly blues at the glassy carbon electrode. Each of the first four waves corresponds to a reversible two-electron transfer. The mixed-valence blue species were characterized by their inherent visible and infrared (IR) spectra.

The so-called Dawson-type heteropolyanion was first reported for $P_2W_{18}O_{62}^{6-}$ by Dawson and then for $P_2Mo_{18}O_{62}^{6-}$ by Strandberg.[1,2] In addition, $As_2W_{18}O_{62}^{6-}$ and $As_2Mo_{18}O_{62}^{6-}$ anions are known to exist.[3,4] These heteropolyanions have been extensively studied with respect not only to the crystal structures and physical properties in the solid state, but also to the chemical natures in the solution state where they are electroreduced in multi-steps to mixed-valence blue species.[5-7] Nowadays, these behaviors are comprehensively explained in relation to those of the corresponding Keggin-type heteropolyanions.[8] However, there are no previous studies on heteropolyanions with SO_4^{2-} as a central tetrahedron because of the lack of proper examples except for the $S_2V_2W_{16}O_{62}^{6-}$ anion.[9]

In the presence of organic solvents such as acetone and acetonitrile, acidified Mo(VI) solutions become pale-yellow due to the formation of $Mo_6O_{19}^{2-}$.[10-13] When H_2SO_4 was used for the acidification, the yellow color became more intense by heating and the resulting orange-yellow solution changed to blue by chemical and electrochemical reductions. These results show strong promise of the formation of a heteropolymolybdosulfate because the reduction of $Mo_6O_{19}^{2-}$ yields a brown solution.[14] Actually, an orange-yellow heteropolyanion was isolated as tetraalkylammonium salts (R_4N^+ salts, R=CH_3, C_2H_5, and n-C_4H_9) from a Mo(VI)/H_2SO_4/CH_3CN system.[15] Recently, the crystal structural analysis demonstrated the existence of the Dawson-type molybdosulfate anion, $S_2Mo_{18}O_{62}^{4-}$ with SO_4^{2-} anions as central tetrahedra.[16]

The present paper describes the chemical and physicochemical properties of the yellow Dawson-type molybdosulfate anion in solutions, regarding to the optimum formation conditions, ultraviolet(UV)-visible spectroscopic characteristics, and electrochemical behaviors. In addition, mixed-valence blue species are identified by visible and IR spectroscopy.

Experimental

Voltammetric measurements were made on a PARC 174-A polarographic analyzer equipped with a Yokogawa Hokushin Electric 3023 X-Y recorder. A Tokai glassy carbon (GC-30S) with a surface area of 0.071 cm^2 was used as a working electrode. Controlled potential electrolysis (CPE) was carried out with a Hokuto Denko HA-501 potentiostat. A Hokuto Denko HF-202D coulometer was used for coulometric experiments. Glassy carbon fibers (GC-20) were employed as a working electrode. A platinum wire was used as a counter electrode and a saturated calomel electrode (SCE) served as the reference electrode. UV-visible spectra were recorded on a Hitachi 220-A spectrophotometer equipped with a constant temperature housing for the cell. UV-visible spectrophotometric and voltammetric measurements were made at 25±0.1 °C. IR spectra were recorded on a Hitachi 270-30 spectrophotometer as KBr pellets. The TG-DTA measurements were carried out with a Rigaku Denki 8002-SD thermal analyzer.

All reagents were of analytical grade and were used without further purification. Molybdenum(VI) solutions were prepared from $Na_2MoO_4 \cdot 2H_2O$.

The Et_4N^+ and n-Bu_4N^+ salts of the yellow molybdosulfate, $(Et_4N)_4S_2Mo_{18}O_{62}$ and $(n\text{-}Bu_4N)_4S_2Mo_{18}O_{62}$ prepared according to ref. 15 were purified further by recrystallization from neat CH_3CN. As already described,[16] the crystals contain the solvent molecule of CH_3CN as a constituent. The TG-DTA analysis for the crystals showed that they lost the CH_3CN molecule around 130 °C via an endothermic process. The crystals were heated at 130 °C for several hours to let the solvent molecule liberate. The fine powders thus obtained were used for preparing solutions of a given concentration of the heteropolyanion.

Results and Discussion

UV-Visible Spectroscopic Measurements. The R_4N^+ salts of the $S_2Mo_{18}O_{62}^{4-}$ anion are soluble in organic solvents such as acetonitrile, acetone, and dimethyl sulfoxide, giving rise to yellow solutions. Curve a of Fig. 1 shows a UV-visible spectrum of 1.98×10^{-5} M (M=mol dm^{-3}) $S_2Mo_{18}O_{62}^{4-}$ in CH_3CN. The complex anion shows a broad absorption band in

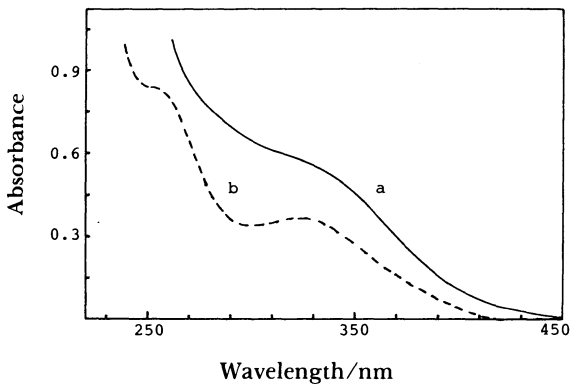

Fig. 1. UV-visible spectra of 1.98×10^{-5} M $S_2Mo_{18}O_{62}^{4-}$ in a, neat CH_3CN and b, 90% (v/v) CH_3CN–water.

the 270—450 nm range. The spectrum in neat CH_3CN was unchanged for at least one month, and conformed to Beer's law in the whole spectral region studied, the molar absorption coefficient at 330 nm being calculated as 2.71×10^3 cm^{-1} M^{-1}.

With the addition of water by more than 5% (v/v), however, the color of the solution changed gradually to pale-yellow. In the presence of 10% (v/v) water, for example, the spectrum was converged in 24 h to that shown in curve b of Fig. 1. The ultimate spectrum with absorption maxima at 257 and 325 nm is attributed not to the reformation of other-type heteropolyanions, but to the hexamolybdate, $Mo_6O_{19}^{2-}$.[11,13] The decomposition was retarded by the presence of 1.0 M $HClO_4$ in the solution, where the spectrum was unchanged for a week. On the basis of these facts, the hydrolytic decomposition of the heteropolyanion proceeds according to the reaction:

$$S_2Mo_{18}O_{62}^{4-} + 3H_2O = 3Mo_6O_{19}^{2-} + 2SO_4^{2-} + 6H^+$$

In the presence of 1.0 M HCl or 1.0 M H_2SO_4 in place of the $HClO_4$, on the other hand, the heteropolyanion decomposed within several hours to give colorless solutions, which is due to the formation of colorless molybdenum(VI)–chloro or molybdenum(VI)–sulfato complexes.[17–19]

Formation of the $S_2Mo_{18}O_{62}^{4-}$ Anion in the Mo(VI)/H_2SO_4/CH_3CN System. In order to confirm the conditions for the formation of the $S_2Mo_{18}O_{62}^{4-}$ anion, absorbance measurements were made for the Mo(VI)/H_2SO_4/CH_3CN system. Firstly, a series of 50 mM Mo(VI) solutions containing 50% (v/v) CH_3CN and various concentrations of H_2SO_4 (0.02—1.2 M) were prepared. When stood for 3 h at 25 °C, the solutions turned to pale-yellow in the H_2SO_4 concentration range 0.04—0.4 M. The absorbances at 410 nm are plotted against the H_2SO_4 concentration and shown in curve a of Fig. 2, where absorbances have a maximum around the H_2SO_4 concentration of 0.06 M. By the addition of R_4NBr to

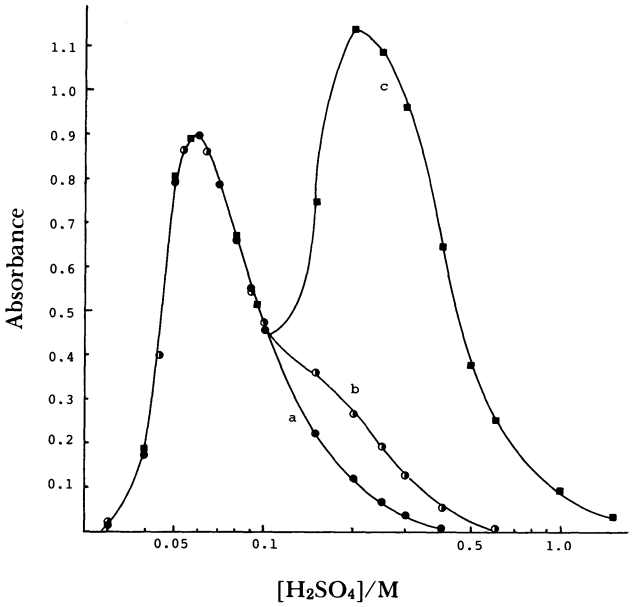

Fig. 2. Absorbances at 410 nm for 50 mM Mo(VI) in 50% (v/v) CH_3CN containing various concentrations of H_2SO_4. Measured after standing a, at 25 °C for 3 h; b, at 25 °C for 24 h; c, at 50 °C for 24 h. Path length, 1 cm.

the solution, pale-yellow precipitates were obtained, being identified as $(R_4N)_2Mo_6O_{19}$ by elemental analysis and IR spectroscopy.[13] When solutions stood for 24 h at 25 °C, absorbances in the H_2SO_4 concentration range >0.2 M were found to increase, while absorbances remained unchanged in the range <0.1 M where $Mo_6O_{19}^{2-}$ was formed. This result, which has been overlooked so far, is well illustrated in curve b. The absorbance grew rather slowly at 25 °C but the absorbance increase was remarkably accelerated by heating of the solution. Curve c shows absorbances after standing at 50 °C for 24 h. Orange-yellow precipitates occurred by the addition of R_4NBr to the yellow solutions in the H_2SO_4 concentration range 0.4—0.8 M. The IR spectrum of the precipitate is in good agreement with that of the authentic $(R_4N)_4S_2Mo_{18}O_{62}$ (vide infra), which indicates that the absorbance increase in the H_2SO_4 concentration range >0.2 M is due to the formation of the yellow $S_2Mo_{18}O_{62}^{4-}$ anion. In conclusion, the $S_2Mo_{18}O_{62}^{4-}$ anion occurs at higher acidities than $Mo_6O_{19}^{2-}$ anion, each anion being distinguishable by the region and condition of formation.

The effect of the Mo(VI) concentration on the complex formation was studied in 50% (v/v) CH_3CN containing 0.4 M H_2SO_4. Absorbances at 400 and 430 nm were measured at 25 °C after standing at 70 °C for 2 h, and plotted against the Mo(VI) concentration in Fig. 3. It was observed that the complex formation became appreciable only at Mo(VI) concentrations >30 mM. Finally, the effect of the CH_3CN concentration (0—80% (v/v)) was investigated. The presence of

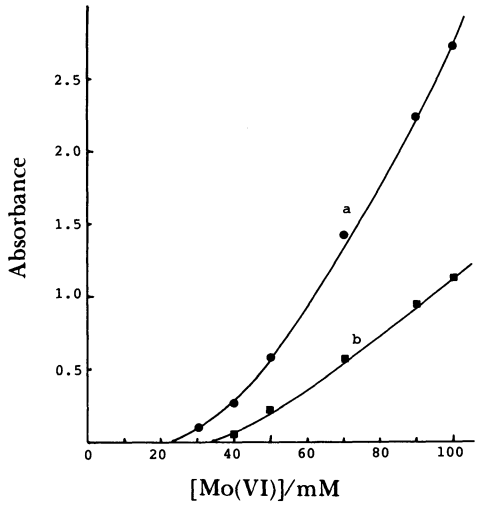

Fig. 3. Effect of Mo(VI) concentrations on absorbances after standing at 70°C for 2 h in 50% (v/v) CH_3CN containing 0.4 M H_2SO_4. Wavelength/nm; a, 400; b, 430. Path length, 1 cm.

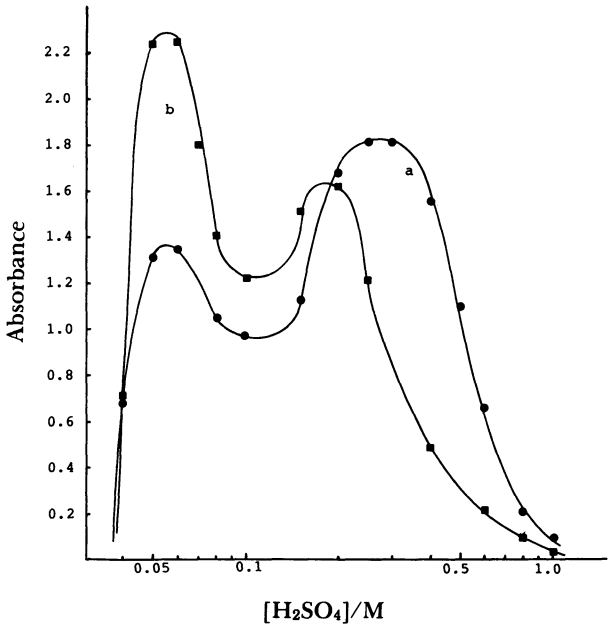

Fig. 4. Absorbances after standing at 50°C for 24 h for 50 mM Mo(VI) in 50% (v/v) a, acetone (400 nm); b, 1,4-dioxane (410 nm) containing various concentrations of H_2SO_4. Path length, a, 2 mm; b, 1 cm.

CH_3CN at concentrations <20% (v/v) had no effect but yellow solutions due to the formation of the $S_2Mo_{18}O_{62}^{4-}$ anion resulted at concentrations >30% (v/v). Adsorbance values increased as the CH_3CN concentration was increased. In the presence of CH_3CN at concentrations >60% (v/v), however, the system separated into two-phases; the $S_2Mo_{18}O_{62}^{4-}$ anion is extracted into the upper layer.

The complex formation is also facilitated in the presence of acetone and 1,4-dioxane. Similar experiments were carried out for the Mo(VI)/H_2SO_4 system containing 50% (v/v) acetone or 1,4-dioxane. The absorbances were measured at 400 nm (for the acetone system) and at 410 nm (for the 1,4-dioxane system) after standing at 50°C for 24 h. The results are illustrated by curves a and b in Fig. 4. Both curves are similar in shape to curve c of Fig. 2, in that the heteropolyanion is formed at higher acidities than $Mo_6O_{19}^{2-}$; the $S_2Mo_{18}O_{62}^{4-}$ anion can be separated from the $Mo_6O_{19}^{2-}$ anion.

Voltammetric Measurements. Figure 5 shows a typical cyclic voltammogram of 8.33×10^{-5} M $S_2Mo_{18}O_{62}^{4-}$ in 95% (v/v) CH_3CN containing 0.1 M $HClO_4$. The voltammogram consists of six cathodic and six anodic waves under these conditions. The peak potentials (E_p's) for the cathodic waves are: +0.53, +0.43, +0.24, −0.06, −0.20, and −0.24 V. Of these, the fifth cathodic wave is observed as a shoulder and the sixth wave is rather unusual in shape. The anodic peaks occurred at +0.55, +0.45, +0.27, −0.04, and −0.18 V; the sixth anodic wave appeared only as a shoulder. The waves are numbered in the direction of more cathodic potentials. For the first four waves, each peak potential is independent of scan rate, v, and each current function $i_p/v^{1/2}$ is constant, i_p being the

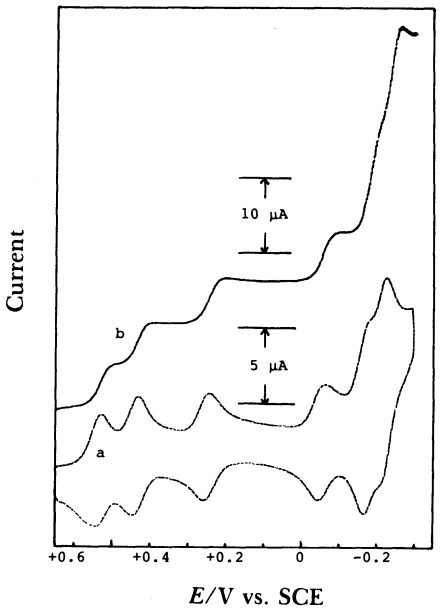

Fig. 5. A cyclic voltammogram (a) and a normal pulse polarogram (b) of 8.33×10^{-5} M $S_2Mo_{18}O_{62}^{4-}$ in 95% (v/v) CH_3CN containing 0.1 M $HClO_4$. Scan rate/mV s^{-1}; a, 100; b, 10.

peak current. The cathodic-to-anodic i_p ratio is one. These results show that each step is diffusion-controlled. The separation of the cathodic and anodic peak potentials for each couple is 28±3 mV, which indicates that these waves are reversible two-electron waves. Coulometric analysis showed that each of the first four reductions consumed two-electrons per the

$S_2Mo_{18}O_{62}^{4-}$ anion. The E_p's shifted to more positive potentials with an increase in the $HClO_4$ concentration. The E_p's for the first four reductions were measured in 95% (v/v) CH_3CN solutions with various concentrations of $HClO_4$ (0.01—0.1 M) which were kept at constant ionic strength of 0.1 with $NaClO_4$. Plots of E_p's against the logarithm of the $HClO_4$ concentration yielded straight lines with a common slope of 60±5 mV, indicating that two protons are consumed for each step of the first four reduction waves.

CPE at each of the first four steps was carried out for 1.0×10^{-4} M $S_2Mo_{18}O_{62}^{4-}$ in 95% (v/v) CH_3CN containing 0.1 M $HClO_4$. Figure 6 shows visible spectra of the solutions obtained. When CPE was made at +0.50 V, a blue solution was obtained, showing a round maximum around 760 nm (curve a). When electrolyzed at +0.35 V, the maximum shifted to 690 nm. As the degree of reduction further proceeded, the blue color became more intense. The spectrum for a 6-electron reduction species was characterized by two maxima around 670 and 790 nm (curve c). Curve d is the spectrum for a 8-electron reduction species, showing a maximum at 570 nm with a round shoulder around 700 nm. Each of 2-, 4-, 6-, and 8-electron reduction species is stable in 95% (v/v) CH_3CN containing 0.1 M $HClO_4$. When reoxidized at +0.80 V, the respective blue species were reverted to the original yellow species, which was identified by IR measurements.

As shown in Fig. 5, the peak separation between the fifth and sixth waves is so small that it is difficult to obtain the visible spectrum for the blue solution by CPE at the fifth step. However, the visible spectrum obtained by CPE at the sixth step (at −0.30 V) was identical in shape with that of the 8-electron reduction species shown in curve d. As CPE at −0.30 V progressed, the spectrum showed a gradual absorbance decrease in the range 450—900 nm. Finally a colorless solution resulted, indicating the decomposition of the heteropolyanion. These observations suggest that the 8-electron reduction species accepts further electrons with the subsequent decomposition.

As shown in curve b of Fig. 5, six reduction waves were observed in normal pulse polarography. Their approximate current ratios are 1:1:1:1:2:2, fitting the 2:2:2:2:4:4 electron ratios. In normal pulse polarography, short potential pulses (57 ms) are applied so that the electrode is at its initial potential most of the time. Therefore the effect of the decomposition may not be observed.

The reduction process of $S_2Mo_{18}O_{62}^{4-}$ is summarized as follows:

$$S_2Mo_{18}O_{62}^{4-} + 2H^+ + 2e = H_2S_2Mo^{V}_2Mo^{VI}_{16}O_{62}^{4-}$$

$$H_2S_2Mo^{V}_2Mo^{VI}_{16}O_{62}^{4-} + 4H^+ + 4e = H_6S_2Mo^{V}_6Mo^{VI}_{12}O_{62}^{4-}$$

$$H_6S_2Mo^{V}_6Mo^{VI}_{12}O_{62}^{4-} + 2H^+ + 2e = H_8S_2Mo^{V}_8Mo^{VI}_{10}O_{62}^{4-}$$

$$H_8S_2Mo^{V}_8Mo^{VI}_{10}O_{62}^{4-} + 4e \longrightarrow \text{unstable species}$$

IR Spectroscopic Measurements. Figure 7 shows IR spectra for Et_4N^+ salts of 2- and 4-electron reduction species in addition to the yellow species. As for the yellow species, as reported previously,[15] bands in the range 1500—1350 cm^{-1} are due to the Et_4N^+ unit, and bands at 1170 and 1070 cm^{-1} can be assigned to the asymmetric and symmetric stretches of the S-O bond. In the Mo-O stretching and bending region (<1000 cm^{-1}), the strong band at 960 cm^{-1} can be assigned to Mo=$O_{terminal}$ bonds. In addition, a weak band at 880 cm^{-1} and a broad band at 785 cm^{-1} are observed. Thouvenot et al. have made a systematic vibrational study of $XMo_{12}O_{40}^{n-}$ salts related to the Keggin

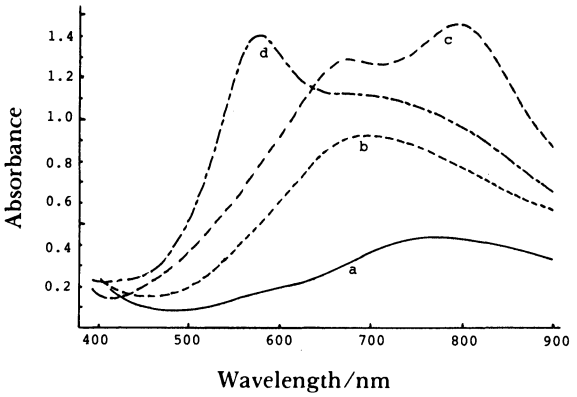

Fig. 6. Visible spectra of the reduced species for 1.0×10^{-4} M $S_2Mo_{18}O_{62}^{4-}$ in 95% (v/v) CH_3CN containing 0.1 M $HClO_4$. a, b, c, d; 2-, 4-, 6-, and 8-electron reduction species, respectively. Path length, 5 mm.

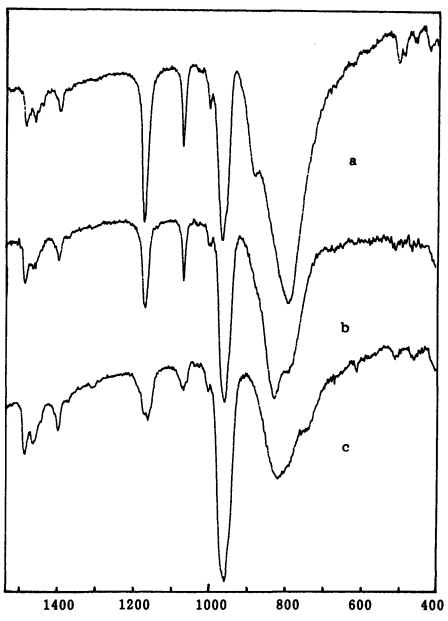

Fig. 7. IR spectra of Et_4N^+ salts of heteropolymolybdosulfates. a, the yellow species; b, 2-electron reduction species; c, 4-electron reduction species.

structure.[20] According to them, bands in the range 890—850 cm^{-1} correspond to inter Mo–O–Mo bridges between corner-sharing octahedra, and bands in the range 800—760 cm^{-1} to intra Mo–O–Mo bridges between edge-sharing octahedra. Both bands at 880 and 785 cm^{-1} are situated within the region predicted by them. In addition to these strong bands, the spectrum contains weak bands at 504, 492, 460, and 420 cm^{-1} to which no assignments can be made.

To obtain the salt of blue species, n-Bu_4N^+ salts of the yellow heteropolyanion were dissolved in 95% (v/v) CH_3CN containing 0.1 M $HClO_4$ and electrolyzed by CPE at +0.50 and +0.35 V. During the electrolysis, the solution was purged with N_2 gas to avoid possible reoxidation by dissolved oxygen. At the end of each electrolysis, Et_4NBr was added to the solution, and the Et_4N-salts of 2- and 4-electron reduction species were obtained. The 4-electron reduction species was also synthesized by CPE of the 0.1 M Mo(VI)/1.5 M H_2SO_4/40% (v/v) CH_3CN system at −0.10 V.[21] As the degree of reduction proceeded, as shown in curves b and c of Fig. 7, both bands due to the S–O bond decreased in intensity with a simultaneous shift to shorter wave numbers. Simultaneously, intensities of bands due to the Mo–O–Mo bridges decreased, while the band due to the $Mo{=}O_{terminal}$ bond remained unchanged. Similar behavior has been reported for the $PMo_{12}O_{40}^{3-}$ salt known as the Keggin structure.[22,23]

References

1) B. Dawson, *Acta Crystallogr.*, **6**, 113 (1953).
2) R. Strandberg, *Acta Chem. Scand.*, **A29**, 350 (1975).
3) F. Kehrmann, *Z. Anorg. Allgem. Chem.*, **22**, 285 (1900).
4) A. Rosenheim and A. Traube, *Z. Anorg. Chem.*, **91**, 75 (1915).
5) M. T. Pope and E. Papaconstantinou, *Inorg. Chem.*, **6**, 1147 (1967).
6) E. Papaconstantinou and M. T. Pope, *Inorg. Chem.*, **6**, 1152 (1967).
7) P. Souchay, R. Contant, and J. Fruchart, *C. R. Acad. Sci.*, **C264**, 976 (1967).
8) L. C. W. Baker and J. S. Figgis, *Inorg. Chem.*, **92**, 3794 (1970).
9) A. Botar and J. Fuchs, *Z. Naturforsch.*, **B37**, 806 (1982).
10) K. Murata, E. Yamamoto, and S. Ikeda, *Bull. Chem. Soc. Jpn.*, **56**, 941 (1983).
11) J. J. Cruywagen and T. Rypstra, *Polyhedron*, **4**, 545 (1985).
12) A. Halasz and E. Pungor, *Talanta*, **18**, 569 (1971).
13) S. Himeno, N. Ishii, M. Hasegawa, A. Saito, and T. Hori, *Inorg. Chim. Acta*, **131**, L11 (1987).
14) M. Che, M. Fournier, and J. P. Launay, *J. Chem. Phys.*, **71**, 1954 (1979).
15) T. Hori and S. Himeno, *Chem. Lett.*, **1987**, 53.
16) T. Hori, O. Tamada, and S. Himeno, *J. Chem. Soc., Dalton Trans.*, in press.
17) S. Himeno and M. Hasegawa, *Inorg. Chim. Acta*, **73**, 255 (1983).
18) S. Himeno, Y. Ueda, and M. Hasegawa, *Inorg. Chim. Acta*, **70**, 53 (1983).
19) E. F. C. H. Rohwer and J. J. Cruywagen, *J. South African Chem. Inst.*, **19**, 11 (1966).
20) R. Thouvenot, M. Fournier, R. Franck, and C. Rocchiccioli-Deltcheff, *Inorg. Chem.*, **23**, 598 (1984); C. Rocchiccioli-Deltcheff, M. Fournier, R. Franck, and R. Thouvenot, *Inorg. Chem.*, **22**, 207 (1983).
21) T. Hori, M. Sugiyama, and S. Himeno, *Chem. Lett.*, **1988**, 1017.
22) H. Tsuneki, H. Niiyama, and E. Echigoya, *Chem. Lett.*, **1978**, 645.
23) K. Eguchi, Y. Toyozawa, K. Furuta, N. Yamazoe, and T. Seiyama, *Chem. Lett.*, **1981**, 1253.